THE JOURNAL OF BIOLOGICAL CHEMISTRY VOL. 283, NO. 34, pp. 23343–23352, August 22, 2008

Structure-guided Mutational Analysis of the OB, HhH, and BRCT Domains of *Escherichia coli* DNA Ligase*[S]

Received for publication, April 17, 2008, and in revised form, May 26, 2008 Published, JBC Papers in Press, May 30, 2008, DOI 10.1074/jbc.M802945200

Li Kai Wang, Pravin A. Nair, and Stewart Shuman[1]

From the Molecular Biology Program, Sloan-Kettering Institute, New York, New York 10021

NAD$^+$-dependent DNA ligases (LigAs) are ubiquitous in bacteria and essential for growth. LigA enzymes have a modular structure in which a central catalytic core composed of nucleotidyltransferase and oligonucleotide-binding (OB) domains is linked via a tetracysteine zinc finger to distal helix-hairpin-helix (HhH) and BRCT (BRCA1-like C-terminal) domains. The OB and HhH domains contribute prominently to the protein clamp formed by LigA around nicked duplex DNA. Here we conducted a structure-function analysis of the OB and HhH domains of *Escherichia coli* LigA by alanine scanning and conservative substitutions, entailing 43 mutations at 22 amino acids. We thereby identified essential functional groups in the OB domain that engage the DNA phosphodiester backbone flanking the nick (Arg^{333}); penetrate the minor grove and distort the nick (Val^{383} and Ile^{384}); or stabilize the OB fold (Arg^{379}). The essential constituents of the HhH domain include: four glycines (Gly^{455}, Gly^{489}, Gly^{521}, Gly^{553}), which bind the phosphate backbone across the minor groove at the outer margins of the LigA-DNA interface; Arg^{487}, which penetrates the minor groove at the outer margin on the 3′-OH side of the nick; and Arg^{446}, which promotes protein clamp formation via contacts to the nucleotidyltransferase domain. We find that the BRCT domain is required in its entirety for effective nick sealing and AMP-dependent supercoil relaxation.

Escherichia coli NAD$^+$-dependent DNA ligase (LigA)[2] exemplifies a family of essential DNA replication/repair enzymes found in all bacteria. LigA catalyzes the sealing of 3′-OH/5′-PO_4 nicks in duplex DNA via a series of three nucleotidyl transfer reactions. (i) LigA reacts with NAD$^+$ in the absence of nucleic acid to form a covalent ligase-(lysyl-*N*-)-AMP intermediate and release NMN; (ii) LigA-AMP binds to nicked duplex DNA and transfers the adenylate from the active site lysine to the 5′-PO_4 terminus to form an adenylylated nicked intermediate, AppDNA; (iii) LigA remains bound to the adenylylated nick and immediately catalyzes the attack of the nick 3′-OH on the 5′-phosphoanhydride linkage, resulting in a repaired phosphodiester and release of AMP (1–3).

All LigA enzymes have a modular structure in which a central ligase catalytic core, composed of a nucleotidyltransferase (NTase) domain (amino acids 70–316 in *E. coli* LigA) and an oligonucleotide-binding (OB) domain (amino acids 317–404), is flanked by an N-terminal "Ia" domain (amino acids 1–69) and three C-terminal modules: a tetracysteine zinc finger domain (amino acids 405–432), a helix-hairpin-helix (HhH) domain (amino acids 433–586), and a BRCA1-like C-terminal (BRCT) domain (amino acids 587–671) (4–8). Each step of the ligation pathway depends upon a different subset of these modules.

Domain Ia is unique to NAD$^+$-dependent ligases and is the determinant of NAD$^+$ specificity (9–11). During the ligase adenylylation reaction, the Ia domain closes over the NAD$^+$ nucleotide bound by the NTase domain, grabs the NMN moiety of NAD$^+$ via multiple contacts to essential amino acids in domain Ia, and thereby orients the NMN leaving group apical to the attacking lysine nucleophile (Lys^{115} in *E. coli* LigA) (6, 10). Recognition of the AMP moiety of NAD$^+$ and the catalysis of nucleotidyl transfer chemistry is accomplished by a constellation of essential amino acid side chains within the NTase domain that contact the adenine base, the ribose sugar, or the α-phosphate of the adenylate (5, 6, 8, 12, 13) (Fig. 1). Most of the essential NTase residues are located within a set of five peptide motifs that define a covalent nucleotidyltransferase superfamily, which includes ATP-dependent DNA ligases, ATP-dependent RNA ligases, and GTP-dependent mRNA capping enzymes (14). An N-terminal fragment of LigA, comprising just the Ia and NTase domains, is competent to catalyze ligase adenylylation (9, 15–18), but it is unable to perform the second and third steps of the pathway. Deleting only the Ia domain from NAD$^+$-dependent ligases abolishes ligase adenylylation without affecting phosphodiester formation at a preadenylylated nick (step 3) (9–11). These results, and others (9, 15, 16, 18, 19), implicate the C-terminal domains of NAD$^+$-dependent ligases in recognition of the DNA substrate.

The crystal structure of *E. coli* LigA bound to the nicked DNA-adenylate intermediate (8) revealed that LigA encircles the DNA helix as a C-shaped protein clamp (Fig. 1). The protein-DNA interface entails extensive DNA contacts by the NTase, OB, and HhH domains over a 19-bp segment of duplex DNA centered about the nick (Fig. 1). The NTase domain binds to the broken DNA strands at and flanking the nick, the OB domain contacts the continuous template strand surrounding the nick, and the HhH domain binds both strands across the minor groove at the periphery of the footprint. The zinc finger module bridges the OB and HhH domains, and it contributes only a single main-chain amide contact to the DNA backbone (8). Domain Ia makes no contacts to the DNA duplex, consist-

* This work was supported, in whole or in part, by National Institutes of Health Grant GM63611. The costs of publication of this article were defrayed in part by the payment of page charges. This article must therefore be hereby marked "*advertisement*" in accordance with 18 U.S.C. Section 1734 solely to indicate this fact.

[S] The on-line version of this article (available at http://www.jbc.org) contains a supplemental figure.

[1] An American Cancer Society Research Professor. To whom correspondence should be addressed: E-mail: s-shuman@ski.mskcc.org.

[2] The abbreviations used are: LigA, NAD$^+$-dependent DNA ligase; OB, oligonucleotide-binding; HhH, helix-hairpin-helix; BRCT, BRCA1-like C-terminal; NTase, nucleotidyltransferase.

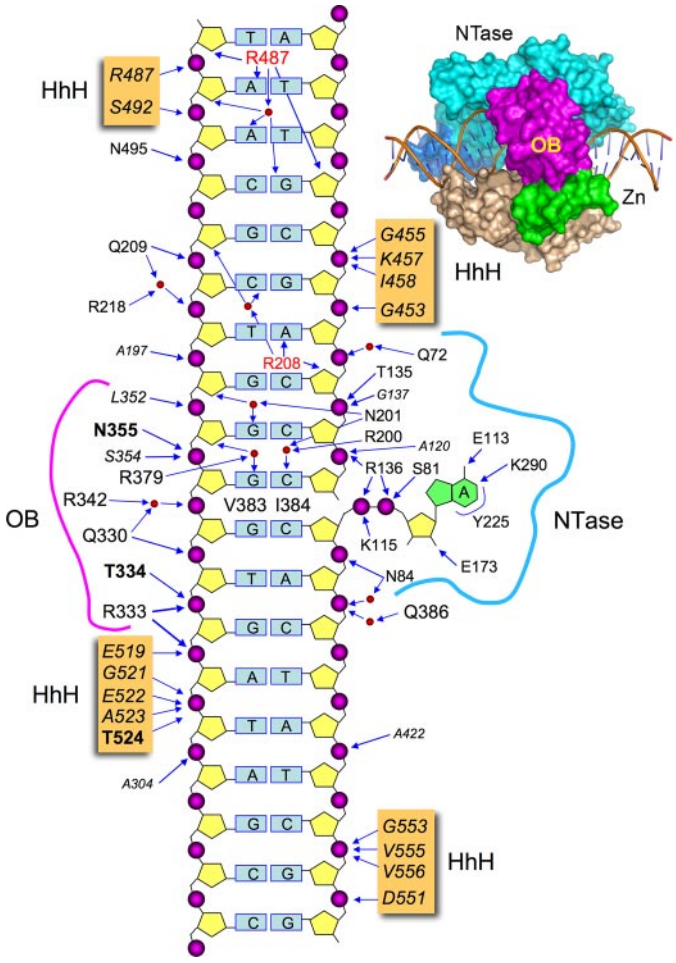

FIGURE 1. **Schematic summary of *E. coli* LigA contacts to DNA.** The nicked duplex DNA is depicted as a two-dimensional schematic, with the continuous template strand on the *left* and the nicked strands on the *right*. The extrahelical 5′-adenylate is shown at *right*. The DNA contacts of LigA side chains (residue identity in *plain text*) and main-chain amides (residue identity in *italics*) are indicated by *arrows*. Amino acids making both main-chain and side-chain contacts to DNA are in *bold font*. Water-mediated interactions are shown with waters as *red spheres*. LigA residues that penetrate the DNA helix and interact with the bases are indicated within the DNA base pair ladder. A space-filling view of LigA bound to nicked DNA-adenylate is shown at the *top right*.

ent with its dispensability for catalysis of strand closure on an AppDNA substrate (10). No electron density was observed for the C-terminal BRCT domain, notwithstanding that the crystals contained full-length LigA and there was empty space in the lattice adjacent to the HhH domain (8). There is a lack of consensus in the literature concerning the necessity and function of the BRCT domain of NAD^+-dependent DNA ligases. The fact that a second *E. coli* LigA paralog (LigB) and two entomopoxvirus ligases have NAD^+-dependent nick sealing activity, although they lack the BRCT domain (9, 20, 21), indicates that this structural module is not a defining requirement for NAD^+-dependent ligation. However, there have been several reports of the effects of deleting the BRCT domain of bacterial or viral LigA proteins, which range from deleterious (11, 22, 23) to mild or minimal (17–19), depending on which LigA enzyme is being investigated.

Here, we used the *E. coli* LigA-DNA crystal structure to guide a mutational analysis of the constituents of the OB and HhH domains that either make atomic contacts to the DNA substrate or are implicated in the formation of the ligase clamp. We thereby defined a suite of amino acid functional groups, distant from the LigA active site, that are essential for nick sealing. We also conducted a deletion analysis and alanine scan of the BRCT domain of *E. coli* LigA guided by an NMR structure of the BRCT domain of *Thermus thermophilus* LigA.[3]

EXPERIMENTAL PROCEDURES

Ligase Mutants—Missense and nonsense mutations were introduced by PCR into the pET-EcoLigA expression plasmid as described previously (12). The entire *ligA* gene was sequenced in every case to confirm the desired mutation and exclude the acquisition of unwanted changes during PCR amplification and cloning. The expression plasmids were transformed into *E. coli* BL21(DE3). Mutant and wild-type ligases were purified from the soluble lysates of isopropyl-1-thio-β-D-galactopyranoside-induced BL21(DE3) cells by nickel-agarose chromatography as described (12). The protein concentrations were determined using the Bio-Rad dye reagent with bovine serum albumin as a standard.

Nick Ligation—Reaction mixtures (20 μl) containing 50 mM Tris-HCl (pH 7.5), 10 mM $(NH_4)_2SO_4$, 5 mM dithiothreitol, 5 mM $MgCl_2$, 20 μM NAD^+, 1 pmol of 5′ ^{32}P-labeled nicked duplex DNA substrate, and aliquots of serial 2-fold dilutions of wild-type or mutant ligases were incubated at 22 °C for 20 min. The products were resolved by electrophoresis through a 15-cm 18% polyacrylamide gel containing 7 M urea in 0.5× TBE (45 mM Tris borate, 1.25 mM EDTA). The extents of ligation were determined by scanning the gel with a Fujix BAS2500 imager. The specific activities of wild-type and mutant ligases were determined from the slopes of the titration curves in the linear range of enzyme dependence. The activities of the mutant ligases were normalized to the specific activity of wild-type LigA protein purified in parallel with that mutant and assayed in a parallel with the same preparation of radiolabeled DNA substrate. On average, the wild-type LigA sealed 26 ± 4.9 fmol of nicks per fmol of input enzyme (average value for 10 different titration experiments with three different preparations of recombinant wild-type LigA).

RESULTS AND DISCUSSION

Alanine Scanning of DNA-binding Residues of the LigA OB Domain—The OB domain of *E. coli* LigA comprises a five-strand antiparallel β barrel plus an α helix (8). The concave surface of the OB barrel nestles up to close to the backbone of the template strand (Fig. 2*A*), donating hydrogen bonds to the phosphodiester oxygens from the Gln^{330}, Arg^{333}, Thr^{334}, and Asn^{355} side chains and the main-chain amides of residues 334, 352, 354, and 355. The template strand interface of the OB domain spans six consecutive phosphates centered about the nick (Figs. 1 and 2*A*).

The OB domain makes additional contacts with the DNA in the minor groove opposite the adenylylated nick (Fig. 2*B*).

[3] G. Sahota, B. L. Dixon, Y. P. Huang, J. Aramini, A. Bhattacharya, D. Monleon, G. V. T. Swapna, C. Yin, R. Xiao, S. Anderson, G. T. Montelione, and R. Tejero, RSCB Protein Data Bank, ID code 1L7B.

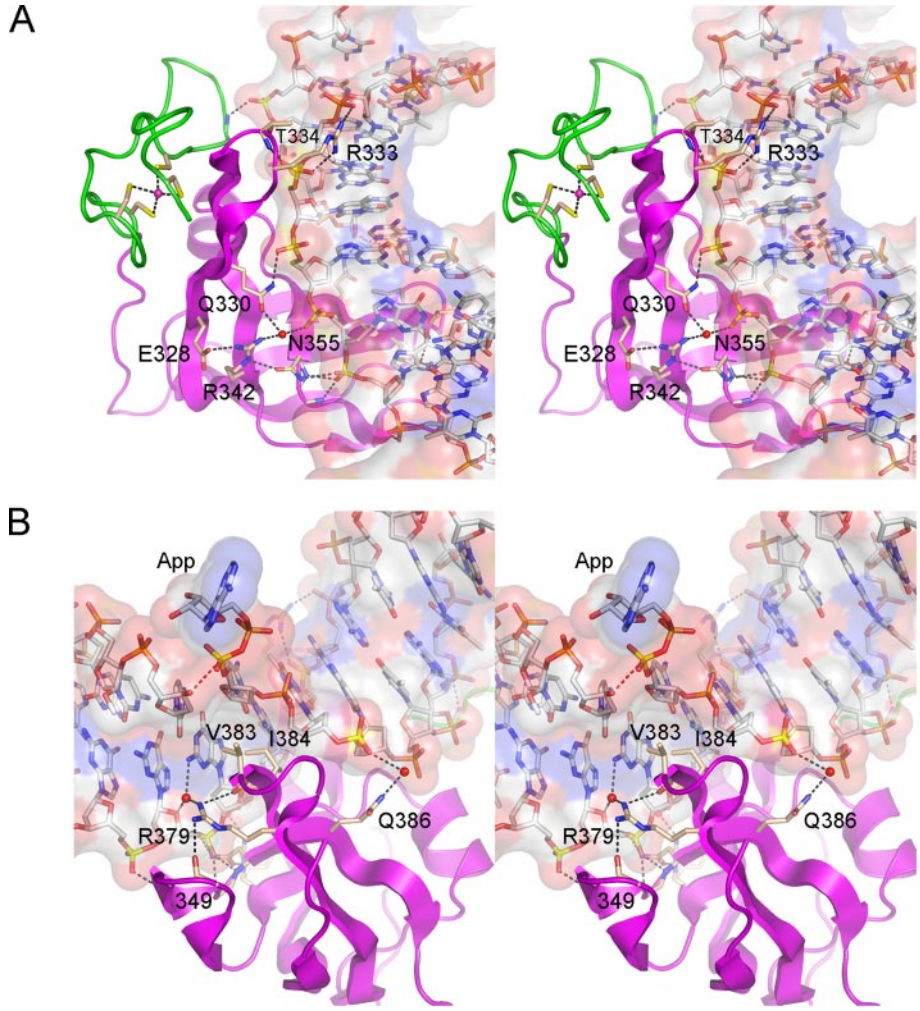

FIGURE 2. **DNA interface of the OB domain.** Shown are stereo views of the OB domain of *E. coli LigA* (colored *magenta*) bound to the nicked DNA, which is rendered as a *transparent surface* over a *stick model*. *A*, this view highlights the concave DNA binding surface of the OB β barrel, which makes numerous contacts with the backbone of the template DNA strand, as shown. The vicinal zinc finger domain is colored *green*. *B*, this view illustrates the penetration of the OB domain into the minor grove opposite the adenylated nick (*App*). The proximity of the nick 3′-O to the nick 5′-phosphorus (3.2 Å) is denoted by the *red dashed line*. Val^{383} and Ile^{384} contact and splay apart the terminal base pairs at the nick. *C*, the amino acid sequence of the *E. coli* LigA OB domain (*Eco*) is aligned to the homologous segments of LigA enzymes from *H. influenzae* (*Hin*), *M. tuberculosis* (*Mtu*), *Bacillus stearothermophilus* (*Bst*), *Staphylococcus aureus* (*Sau*), *Enterococcus faecalis* (*Efa*), *T. filiformis* (*Tfi*), mimivirus (*Mimi*), and entomopoxvirus (*EPV*). Residues targeted for mutational analysis in *E. coli* LigA are indicated by *filled circles* above the sequence. Conservation of the targeted residues is highlighted in *shaded boxes*.

To probe whether any of the aforementioned side chain contacts to DNA are functionally relevant, we introduced single-alanine substitutions for Gln^{330}, Arg^{342}, Asn^{355}, Arg^{379}, and Gln^{386}. Double-alanine changes were introduced at vicinal residues Arg^{333}–Thr^{334} and Val^{383}–Ile^{384}. The wild-type and mutated *E. coli* LigA proteins were produced as N-terminal His_{10} fusions and purified in parallel from soluble bacterial extracts by nickel-agarose chromatography (Fig. 3*A*, *left panel*). The extent of ligation of singly nicked 3′-OH/5′PO_4 DNA by wild-type LigA and each mutant was gauged as a function of input enzyme, and the specific activities were normalized to the wild-type value (defined as 100%). Our operational definition of an important amino acid (or dipeptide) was one at which alanine substitution reduced nick sealing activity to $\leq$10% of the wild-type level. By this criterion, the Arg^{333}–Thr^{334} dipeptide, Arg^{379}, and the Val^{383}–Ile^{384} dipeptide were deemed essential for ligation (Fig. 3*B*, *left panel*). An alignment of the primary structures of the OB domains of LigA enzymes from various bacterial genera (including *Haemophilus*, *Mycobacterium*, *Bacillus*, *Staphylococcus*, *Enterococcus*, and *Thermus*) and eukaryal DNA viruses (mimivirus and entomopoxvirus) reveals that the Arg^{333}, Arg^{379}, Val^{383}, and Ile^{384} side chains are conserved in all of the LigA proteins (Fig. 2*C*). Thr^{334} is conserved in the LigA enzymes from bacteria, with the exception of *Thermus filiformis* (Fig. 2*C*).

By contrast, the alanine mutation at Gln^{330} (which is not conserved in the LigA family; Fig. 2*C*) had no apparent effect on nick sealing, signifying that the bifurcated direct and water-mediated contacts of the Gln^{330} amide group to two of the phosphates of the template DNA strand (Fig. 2*A*) are not important for activity. The Q386A mutant had one-third the activity of wild-type LigA (Fig. 3*B*); thus, the water-mediated contact from Gln Nϵ to the phosphodiester backbone (Fig. 2*B*) might contribute modestly, although not enough to meet our criterion of significance. In addition to this DNA contact, the Gln^{386} Oϵ engages in a hydrogen bond with the Arg^{379} side

Val^{383} and Ile^{384} project into the minor groove and make van der Waals interactions with the terminal cytosine bases on either side of the nick and the penultimate pentose sugar on the 5′ side of the nick. Arg^{379} makes water-mediated contacts in the minor groove to the base and sugar of the two template strand nucleosides flanking the 3′-OH at the nick. Gln^{386} makes a water-mediated contact to the 5′-PO_4 strand (Fig. 2*B*).

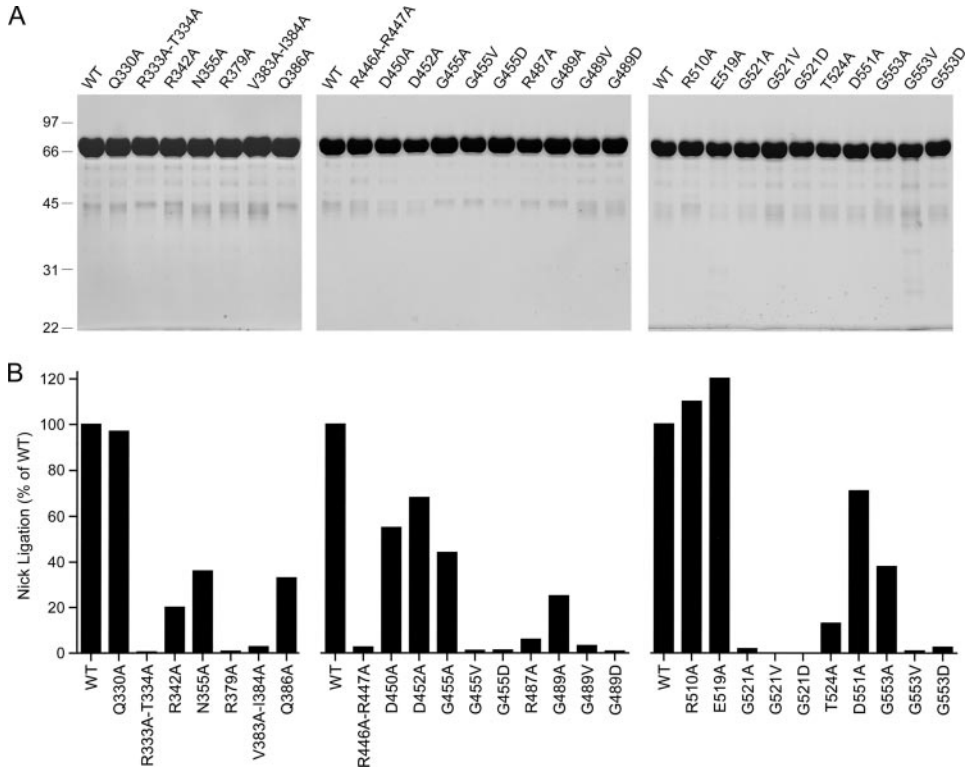

FIGURE 3. **Mutational analysis of the DNA-binding residues of the OB and HhH domains.** *A*, aliquots (8 μg) of the nickel-agarose preparations of wild-type (*WT*) LigA and the indicated alanine mutants were analyzed by SDS-PAGE. The Coomassie Blue-stained gels are shown. The positions and sizes (kDa) of marker polypeptides are indicated on the *left*. *B*, the specific activities of the mutant LigA proteins in nick sealing were determined by enzyme titration and normalized to that of wild-type LigA purified and assayed in parallel with the mutants.

chain emanating from the neighboring β strand (not shown); loss of this contact might contribute to the activity decrement of the Q386A mutant. Gln^{386} is conserved as glutamine or glutamate in all of the bacterial LigA proteins but is replaced by tyrosine or isoleucine in the viral LigA clade (Fig. 2*C*).

Eliminating Asn^{355} and its amide hydrogen bond to a phosphate on the template strand (Fig. 2*A*) reduced nick sealing to one-third the wild-type level (Fig. 3*B*). It is conceivable that the effects of the N355A change are modest because the same phosphate receives functionally redundant hydrogen bonds from the main-chain amides of Asn^{355} and its neighbor Ser^{354} (Fig. 2*A*). It is also possible that the 3-fold activity decrement of the N355A mutant reflects the loss of the hydrogen bond interaction with Arg^{342} in the neighboring strand of the β sheet (Fig. 2*A*), rather than loss of phosphate contacts. Arg^{342} itself participates in the same water-mediated phosphate contact as Gln^{330} Oϵ (Fig. 2*A*). The 5-fold decrement in nick sealing caused by the R342A change (Fig. 3*B*) better mimics the effects of N355A than Q330A, which implies that the role of Arg^{342} might be to stabilize the OB β sheet (via its contacts to Asn^{355} on one side and Glu^{328} on the other; Fig. 2*A*). The Arg^{342}–Asn^{355} pair is confined to *E. coli* LigA (Fig. 2*C*); a similar Lys–Asn pair is present in *Haemophilus influenzae* LigA, but all other aligned LigA enzymes have diverse substitutions at the equivalent positions.

Structure-Activity Relationships at Key Residues of the OB Domain—To refine the structure-function map of the OB domain, we introduced single-alanine changes at the essential Arg^{333}–Thr^{334} dipeptide (Fig. 4*A*). The specific activities of R333A and T334A were 0.8 and 21% of wild-type LigA, respectively (Fig. 4*B*). Thus, Arg^{333} is essential by our criterion, but Thr^{334} is not. The Thr^{334} Oγ donates a hydrogen bond to a nonbridging phosphate oxygen atom of the same phosphodiester coordinated by Arg^{333} (which engages the other nonbridging oxygen). The substantial residual activity of T334A could reflect functional redundancy of the missing Oγ hydrogen bond with the hydrogen bond donated to the same phosphate oxygen by the Thr^{334} main-chain amide (Fig. 2*A*).

The essential Arg^{333} side chain was substituted conservatively by lysine and glutamine (Fig. 4*A*). The finding that lysine resulted in significant gain of activity (to 22% of wild type), whereas glutamine did not (0.8%), attests to the importance of positive charge and the ionic interactions with the phosphate backbone seen in the crystal structure (Fig. 2). The eukaryal viral LigA proteins naturally have lysine in place of the Arg^{333} side chain conserved among bacterial LigA proteins (Fig. 2*C*).

The OB fold Arg^{379} residue defined as essential by the initial alanine scan was also replaced conservatively by lysine and glutamine (Fig. 4*A*). Although lysine afforded some recovery of function when compared with the R379A mutant (6.3% *versus* 0.7% of wild type, respectively), the R379K protein still satisfied our criterion for a significant mutational impairment. Glutamine (1.2% activity) had no salutary effect. We surmise that positive charge at position 379 does not suffice for nick sealing activity, which depends specifically on arginine, a residue that can form multidentate hydrogen bond contacts. Indeed, the crystal structure shows that Arg^{379} not only makes a water-mediated contact to adjacent nucleosides of the template strand (Figs. 1 and 2*B*), it donates hydrogen bonds from its terminal guanidinium nitrogens to main-chain carbonyls of Ala^{349} and Val^{383} (Fig. 2*B*). Ala^{349} is located at the tip of the hairpin turn linking two of the flanking β strands of the OB barrel that pack tightly against the DNA (Fig. 2*B*). We infer that Arg^{379} is needed to stabilize the OB fold in a proper conformation for productive DNA binding. Arg^{379} is conserved in bacterial LigA proteins but is replaced by lysine in the viral homologs (Fig. 2*C*).

The essentiality of the Val^{383}–Ile^{384} dipeptide was especially interesting given their location in the DNA minor groove (Fig. 2*B*). Val^{383} and Ile^{384} engage in an extensive network of van der Waals contacts with the nucleosides flanking the nick (illustrated in supplemental Fig. S1). Val^{383} abuts the C:G base pair at the 3′-OH nick terminus, making van der Waals contacts from Cγ1 to cytosine O2 (3.49 Å) and guanine N2 (3.61 Å) (supple-

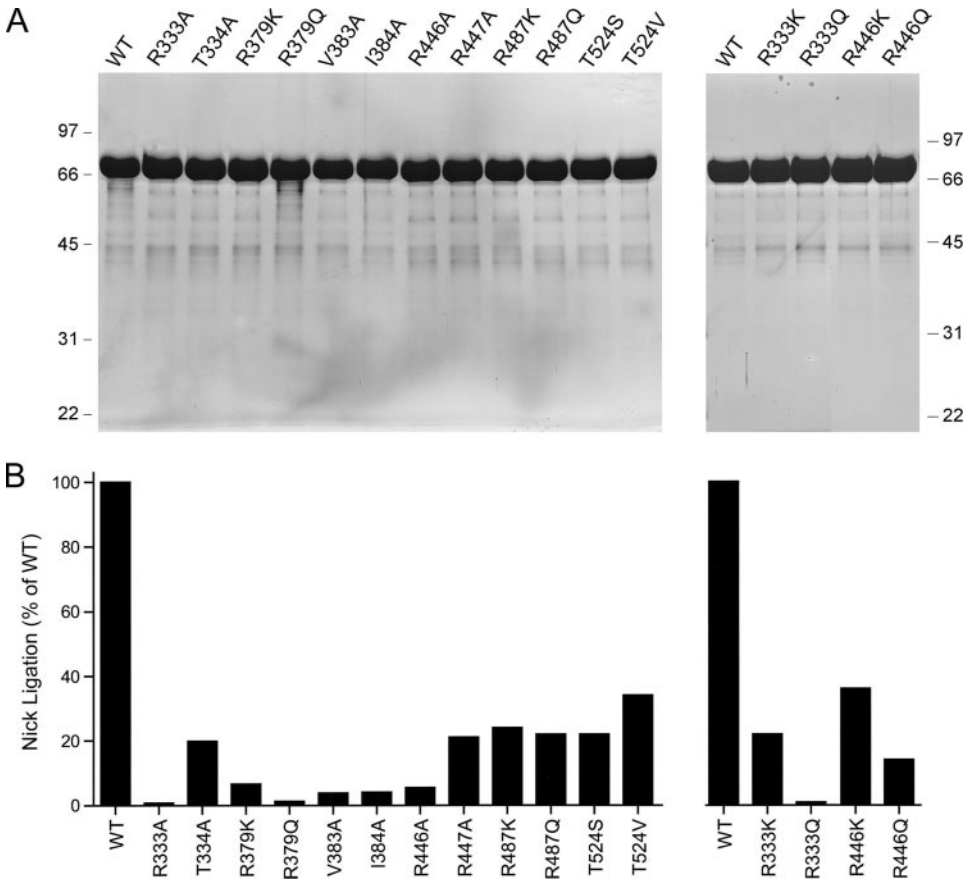

FIGURE 4. **Structure-activity relationships.** *A*, aliquots (8 μg) of the nickel-agarose preparations of wild-type (*WT*) LigA and the indicated mutants were analyzed by SDS-PAGE. The Coomassie Blue-stained gels are shown. The positions and sizes (kDa) of marker polypeptides are indicated on the *left* and *right*. *B*, the specific activities of the mutant LigA proteins in nick sealing were determined by enzyme titration and normalized to that of wild-type LigA purified and assayed in parallel with the mutants.

mental Fig. S1). Ile^{384} stacks on the same guanine base so that the Ile Cδ contacts guanine N2 (3.67 Å) and C4 (3.67 Å). Ile^{384} also nestles against the 5′-terminal C:G base pair of the nick such that cytosine O2 is 3.28 Å from Ile^{384} Cδ and guanine N2 is proximal to Ile^{384} Cδ (3.73 Å), Cγ1 (3.8 Å), and Cγ2 (3.92 Å). In addition, Ile^{384} packs against the penultimate nucleoside sugar of the 5′-PO_4 nick strand, with van der Waals contacts from Ile^{384} Cγ1 to the deoxyribose O4 (3.06 Å) and C5 (3.94 Å) and from Ile^{384} Cβ to the deoxyribose O4 (3.32 Å) and C4 (3.95 Å) (supplemental Fig. S1). The single-alanine mutants V383A and I384A (Fig. 4*A*) were both defective for nick sealing, with 4% of wild-type activity (Fig. 4*B*).

The mutational effects at Val^{383} and Ile^{384} support their imputed role in deforming the local structure of the DNA duplex surrounding the nick (8). The two base pairs flanking the nick on the 3′ side and the base pair at the nick 5′ terminus adopt an RNA-like A helical conformation. Also, the inclination and twist angles between adjacent base pairs exhibit an abrupt distortion at the nick termini, which results in bending and unwinding of the double helix and widening of the major groove surrounding the nick. The contacts of Val^{383} and Ile^{384} with the nucleosides in the minor groove at the nick were proposed to be a principal factor in splaying apart the bases (8). The present mutational data suggest that this OB-induced distortion is a necessary component of the ligation pathway and are in accord with findings that *Thermus* LigA is sensitive to perturbations of the nick 3′-OH base pair in the minor groove (24).

Effects of Mutations at DNA-binding Residues of the LigA HhH Domain—The HhH domain of *E. coli* LigA anchors the phosphodiester backbone at four points that are arrayed symmetrically with respect to the nick (Fig. 5*A*). The LigA HhH domain consists of two tandem $(HhH)_2$ modules, each composed of five α helices, arranged with pseudo two-fold symmetry in the LigA structure. The four-point binding of the HhH domain at the periphery of the LigA-DNA footprint stabilizes a 10° DNA bend centered at the nick. The functional DNA binding units of the *E. coli* LigA HhH domain are the four "loop-helix" motifs: ^{452}DGMGDKI^{458}, ^{487}RMGPKS^{492}, ^{519}EVGEAT^{524}, and ^{551}DVGIVV^{556}. Each binds to a NpNpN trinucleotide via a network of hydrogen bonds from backbone amide nitrogens to the phosphate oxygens of the NpNpN element. The proximal phosphate (5′-N**p**NpN) fits into an oxyanion hole formed by the amino acids at the N terminus of the α helix, which lacks a helix-capping side chain because each helix initiates with a conserved glycine (Gly^{455}, Gly^{489}, Gly^{521}, or Gly^{553}) that contributes to the oxyanion hole (Fig. 1). The adjacent phosphate (5′-NpN**p**N) receives a hydrogen bond from the backbone amide of a hydrophilic amino acid in the loop located two or three residues upstream of the conserved glycine. In *E. coli* LigA, these polar side chains (Asp^{452}, Arg^{487}, Glu^{519}, or Asp^{551}) straddle or penetrate into the DNA minor groove. In particular, Arg^{487} projects deeply into the minor groove, where it makes multiple direct and water-mediated hydrogen bonding contacts to the bases and the sugar atoms of both DNA strands (Fig. 1).

To assess whether the oxyanion holes are functionally important, we introduced the aliphatic chains Ala and Val in lieu of Gly^{455}, Gly^{489}, Gly^{521}, and Gly^{553}. We also replaced the glycines with aspartates, thereby creating the potential for electrostatic repulsion between each of the HhH loop-helix motifs and the DNA phosphodiester backbone. The 12 Gly-to-Ala/Val/Asp mutants of LigA were purified (Fig. 3*A*) and then tested for nick sealing in parallel with wild-type LigA (Fig. 3*B*). In the ^{452}DGM**G**DKI^{458} loop-helix motif that contacts the 3′-OH DNA strand (Fig. 1), changing Gly^{455} to alanine was well tolerated (44% activity), but nick sealing was suppressed 100-fold by valine or aspartate. Modeling a valine or aspartate side chain into the LigA-DNA crystal structure (without modifying the

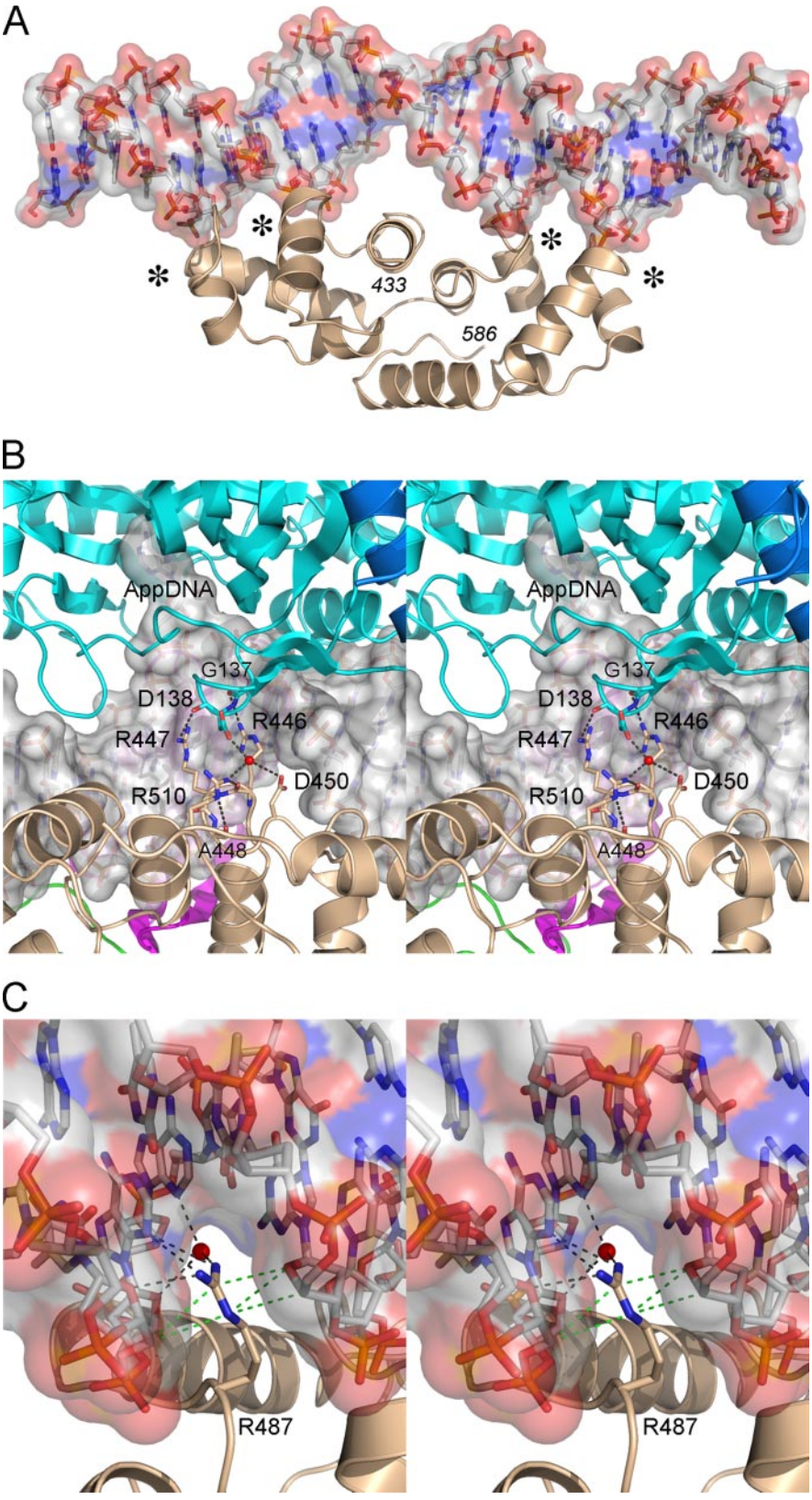

FIGURE 5. **The HhH domain of LigA.** *A*, ribbon diagram of the *E. coli* LigA HhH domain bound to nicked duplex DNA, which is shown as a *semitransparent surface*. The four loop-helix motifs that bind the backbone across the minor groove are indicated by an *asterisk*. *B*, stereo view of the clamp-closing contacts between amino acids in the HhH (*beige*) and NTase (*cyan*) domains of *E. coli* LigA. The interactions occur within the DNA major groove opposite the nick. The DNA is rendered as a *transparent surface* over a *stick model*. *C*, detailed stereo view of the DNA contacts of Arg^{487}, which penetrates the minor groove and makes direct and water-mediated hydrogen bonds (*black dashed lines*) and van der Waals interactions (*green dashed lines*) with nucleobases and deoxyribose sugars.

position of the polypeptide main chain) reveals a severe steric clash between the valine or aspartate side chain and the phosphate in the oxyanion hole (not shown). Although alanine would also impinge on the phosphate when modeled into the crystal structure (albeit less so than valine or aspartate), the biochemical data show that one extra methyl group can be accommodated without much effect on sealing, perhaps by a compensatory local adjustment in the main chain of the loop in the loop-helix motif.

The ^{487}RM**G**PKS^{492} motif contacts the template strand on the 3′-OH side of the nick (Fig. 1). We found that the G489A protein retained one-fourth of wild-type activity, whereas G489V and G489D had 3.2 and 0.8% of wild-type activity, respectively (Fig. 3*B*). The ^{551}DV**G**IVV^{556} motif binds to the 5′-PO_4 DNA strand (Fig. 1). Although G553A had 38% activity, G553V and G553D were reduced to 0.9 and 2.6% activity, respectively (Fig. 3*B*). The loop-helix motif ^{519}EV**G**EAT^{524}, which binds to the template DNA strand on the 5′-PO_4 side of the nick (Fig. 1), was uniquely sensitive to alanine substitution at the glycine of the oxyanion hole. The G521A mutant was 50-fold less active than wild-type LigA, and the G521V and G521D proteins had <0.1% of wild-type function (Fig. 3*B*). Modeling the mutations into the LigA-DNA crystal structure indicated that the valine and aspartates clashed with the bound DNA in each of the oxyanion holes, as did alanines (to a lesser extent). It is not obvious why Gly^{521} was especially affected by the alanine mutation. It is possible that LigA is less able to adapt to the G521A change by adjusting the local main-chain conformation. We surmise from these results that each of the four DNA-binding oxyanion holes of the HhH is important for *E. coli* LigA function.

We also tested the effects of alanine substitutions at the four polar residues (Asp^{452}, Arg^{487}, Glu^{519}, or

Asp[551]) of the respective loop-helix motifs positioned near or in the minor groove. The D452A, E519A, and D551A mutants (Fig. 3*A*) were 68, 120, and 71% as active as wild-type LigA, respectively (Fig. 3*B*), signifying that none of these acidic residues are important for nick sealing. By contrast, changing Arg[487] to alanine reduced activity to 6% of wild type (Fig. 3*B*). Conservative substitutions with lysine and glutamine (Fig. 4*A*) each restored activity to one-fourth of the wild-type level (Fig. 4*B*). We surmise from the mutational effects that Arg[487] makes important hydrogen-bonding interactions. Indeed, the crystal structure shows that Arg[487] penetrates deep into the minor groove and donates multiple hydrogen bonds to the nucleosides of the 5′-AAT trinucleotide of the template strand on the 3′-OH side of the nick (Figs. 1 and 5*C*), specifically from Arg[487] NH2 to the thymidine deoxyribose O4′ and adenine N3 (5′-A**A**T) and from Arg[487] NH1 to the same adenine N3 (5′-A**A**T). Arg[487] makes water-mediated contacts with the adenosine deoxyribose O4′ (5′-A**A**T) and adenine N3 (5′-**A**AT) (Fig. 5*C*). Arg[487] also makes van der Waals interactions with deoxynucleoside sugars of both DNA strands lining the minor groove (Fig. 5*C*). Either lysine or glutamine could sustain the van der Waals contacts and some of the hydrogen-bonding interactions of Arg[487], thereby accounting for their ability to restore function partially. Arg[487] is either conserved or replaced by lysine in other bacterial LigA proteins (Fig. 5*C*).

Thr[524] in the [519]EVGEAT[524] loop-helix motif donates a hydrogen bond from Oγ to a nonbridging oxygen of the phosphate in the oxyanion hole. This is the only instance in the crystal structure of a contact of a side chain of the HhH domain with a DNA phosphate group. The main-chain amide of Thr[524] also donates a hydrogen bond to the same nonbridging phosphate oxygen. Replacing Thr[524] with alanine reduced nick sealing activity to 13% of wild type (Fig. 3*B*). Although this effect did not meet our cut-off criterion, we proceeded to test conservative serine and valine mutations and found that they increased activity to 48 and 38% of wild type, respectively (Fig. 4*B*).

Probing the Role of Interdomain Contacts of the HhH Domain Implicated in Clamp Closure—Although the formation of the LigA clamp is driven by the numerous DNA contacts discussed above, it also involves osculating interactions between the NTase domain and HhH domain (Fig. 5*B*). A detailed view of these contacts shows that they occur in the DNA major groove opposite the nick, where Arg[446] and Arg[447] of the HhH domain donate hydrogen bonds to the backbone carbonyls of NTase residues Gly[137] and Asp[138], and there is a network of water-mediated hydrogen bonds between the Asp[138], Arg[510], and Asp[450] side chains (Fig. 5*B*). To address the functional significance of these contacts, the HhH domain residues Asp[450] and Arg[510] were replaced individually by alanine (Fig. 3*A*). The R510A mutant was fully competent in nick sealing, and the D450A mutant was 55% as active as wild-type LigA. It was reported previously that changing Asp[138] to alanine had only a mild effect on nick sealing activity *in vitro* (38% of wild type) and did not affect LigA activity *in vivo* (13). Thus, the water-mediated contacts of Asp[540] and Arg[510] to Asp[138] are not functionally important.

The Arg[446]–Arg[447] dipeptide was doubly substituted with alanine (Fig. 3*A*). This change elicited a 40-fold decrement in ligation (Fig. 3*B*). We then purified the R446A and R447A single mutants (Fig. 4*A*); their specific activities were 5.4 and 21% of wild-type LigA, respectively (Fig. 4*B*). We surmise that Arg[446] is critical *per se* for optimal nick sealing activity via its promotion of clamp closure. Although the mutational effects at Arg[447] did not meet our criterion of significance, the 5-fold activity decrement of R447A suggests that its contacts to the NTase domain provide some added clamp stability. Structure-activity relations at Arg[446] were obtained by testing conservative substitutions with lysine and glutamine (Fig. 4*A*). Lysine restored activity to 36% of wild type, whereas glutamine afforded 14% of wild-type function. These results suggest that hydrogen bonding is the relevant property of Arg[446], consistent with its contacts to the main chain of the NTase domain. Note that neither Arg[446] nor Arg[447] contacts the DNA in the crystal structure.

Incremental Deletions of the BRCT Domain—Electron density for the BRCT domain was not visible in the crystals of DNA-bound *E. coli* LigA (8). The BRCT domain was also not visualized in the crystal structure of *T. filiformis* LigA (see corrected Protein Data Bank code 1V9P). A solution NMR structure of the isolated BRCT domain of *T. thermophilus* LigA is available in the Protein Data Bank.[3] The LigA BRCT fold comprises a four-strand parallel β sheet overlaid by three α helices (Fig. 6). Because the primary structures of the *T. thermophilus* and *E. coli* LigA BRCT domains are well conserved (37/79 positions of side chain identity plus 12/79 positions of side chain similarity; Fig. 6*A*), we regard the NMR structure of the *T. thermophilus* BRCT domain (Fig. 6*B*) as a surrogate for the homologous *E. coli* module and have exploited it to guide a mutational analysis. Initially, we generated three serial C-terminal truncations, LigA-(1–661), LigA-(1–643), and LigA-(1–636), designed to cleanly delete secondary structure elements of the BRCT domain (Fig. 6*A*). We also constructed a complete deletion of the BRCT domain, LigA-(1–586), that reprises the form of *E. coli* LigA that was visible in the DNA-bound crystal structure (8). The wild-type and truncated proteins were produced as His-tagged derivatives and displayed the expected decrements in size when analyzed by SDS-PAGE (not shown). Complete deletion of the BRCT domain reduced specific activity in nick sealing by LigA-(1–586) to 0.14% of the wild-type value (not shown). The specific activities of the LigA-(1–661), LigA-(1–643), and LigA-(1–636) proteins were $\leq$0.1% of the wild-type LigA activity (not shown). Thus, deletion of all or part of the BRCT domain elicits the same three order of magnitude decrement in nick sealing.

Our findings concerning the essentiality of the BRCT domain for *E. coli* LigA activity agree with previous conclusions concerning the critical role of the BRCT domain in LigA enzymes from *Mycobacterium tuberculosis*, *Thermus* species AK16D, and mimivirus (11, 22, 23). However, our results disagree with the report of Wilkinson *et al.* (19) that deletion of the BRCT domain of *E. coli* LigA resulted in only a 3-fold decrement in the rate of nick sealing by the LigA-(1–592) protein, when compared with their wild-type LigA enzyme. Their LigA enzymes, like ours here, were produced as N-terminal His_{10} fusions. The nicked DNA substrates used in the two studies are similar, except that their substrate contained a fluorescein tag at the 5′ end of the 3′-OH strand. To our inspection, the key

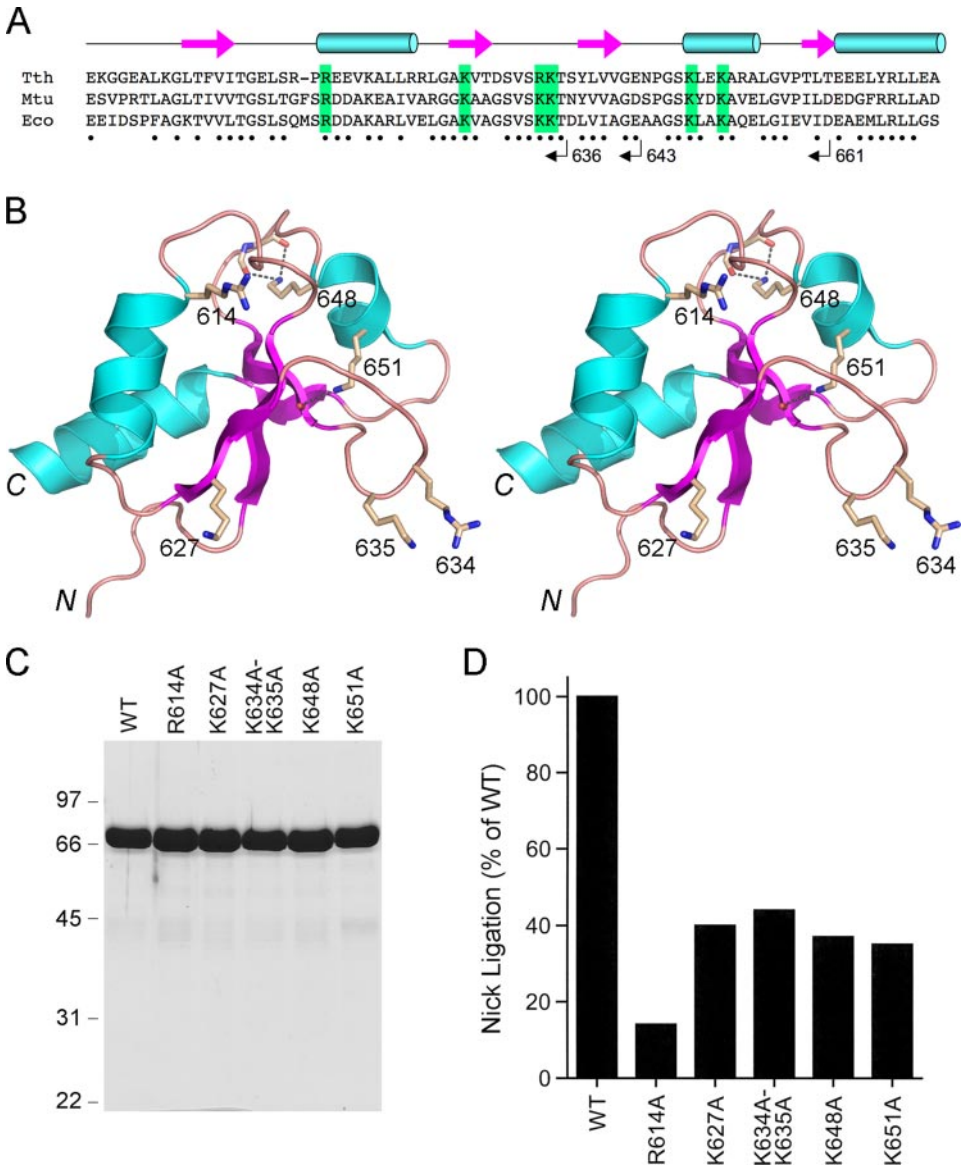

FIGURE 6. **Mutational analysis of the BRCT domain of LigA.** *A*, the amino acid sequence of the *E. coli* LigA BRCT domain (*Eco*) is aligned to the homologous segments of LigA enzymes from *M. tuberculosis* (*Mtu*) and *T. thermophilus* (*Tth*). The secondary structure elements of the TthLigA BRCT domain are displayed above the sequence, with β strands depicted as *arrows* and α helices depicted as *cylinders*. Positions of side-chain identity/similarity between TthLigA and EcoLigA BRCT domains are indicated by *dots* below the sequence. The C termini of serially deleted versions of EcoLigA studied herein are indicated below the sequence. Conserved basic amino acids that were subjected to alanine scanning are highlighted in *green boxes*. *B*, stereo view of the NMR structure of the TthLigA BRCT domain (Protein Data Bank code 1L7B). The side chains equivalent to those chosen for mutational analysis in EcoLigA are shown as *sticks* and labeled with the EcoLigA residue numbers. *C*, aliquots (8 μg) of the nickel-agarose preparations of wild-type (*WT*) LigA and the indicated mutants were analyzed by SDS-PAGE. The Coomassie Blue-stained gel is shown. The positions and sizes (kDa) of marker polypeptides are indicated on the *left*. *D*, the specific activities of the mutant LigA proteins in nick sealing were determined by enzyme titration and normalized to that of wild-type LigA purified and assayed in parallel with the mutants.

difference between the two studies is that their wild-type LigA nick sealing rate (0.1 min^{-1}), measured at nearly equimolar concentrations of enzyme (3.5 μM) and nicked DNA (5 μM), was about 13-fold less than our LigA activity (26 fmol ligation/fmol enzyme/20 min), calculated from the slope of a LigA titration curve under conditions of DNA excess at much lower DNA concentrations (50 nM). We have measured the rate of nick sealing by our LigA preparation at equimolar concentrations of enzyme and nicked DNA (50 nM); the reaction attained 67% of the end point value in 10 s (shorter reaction times were not tested). The calculated turnover number of 3.4 min^{-1} under these conditions was some 30-fold higher than that observed by Wilkinson *et al.* (19). Given the widely posited role for the LigA BRCT domain in DNA binding (11, 16, 17, 19, 22, 23), we surmise that the use of 100-fold higher concentrations of DNA and ΔBRCT protein by Wilkinson *et al.* (19) might have mitigated the impact of the domain deletion in the sealing assay. This factor, and the comparatively feeble activity of their wild-type LigA preparation, could account for the disparity between their results and ours concerning the impact of BRCT deletions.

Effects of BRCT Deletions on AMP-dependent Supercoil Relaxation Suggest a Role in DNA Binding—The structure of DNA-bound *E. coli* LigA (8) shows that the nick is covered completely by the NTase and OB domains (Fig. 1). Thus, the widely invoked role of the BRCT domain in DNA binding by LigA cannot be via direct nick recognition. Rather, the BRCT domain might enhance DNA affinity by: (i) promoting closure of the protein clamp around the duplex, via interdomain interactions, and/or (ii) contacting the DNA flanking the nick. To gauge the contributions of the BRCT domain to duplex DNA binding, we turned to an assay of LigA-catalyzed relaxation of DNA supercoils (25). This assay takes advantage of the microscopic reversibility of step 3 of the ligation reaction, whereby ligase apoenzyme can, in the presence of high concentrations of AMP and a divalent cation, catalyze attack by an AMP phosphate oxygen on the DNA phosphodiester backbone to form a nicked DNA-adenylate that is then resealed by forward catalysis of step 3. If the starting DNA substrate is a covalently closed supercoiled circular plasmid DNA, and if ligase releases the 3′-OH end of the AppDNA nick before executing forward step 3, the net result is incremental supercoil relaxation.

Full-length LigA relaxed negatively supercoiled plasmid DNA in the presence of 10 mM AMP to generate a mixture of partially relaxed topoisomers and fully relaxed circles plus a minor fraction of nicked circular products (Fig. 7). No supercoil relaxation by LigA was detected when AMP was omitted (data

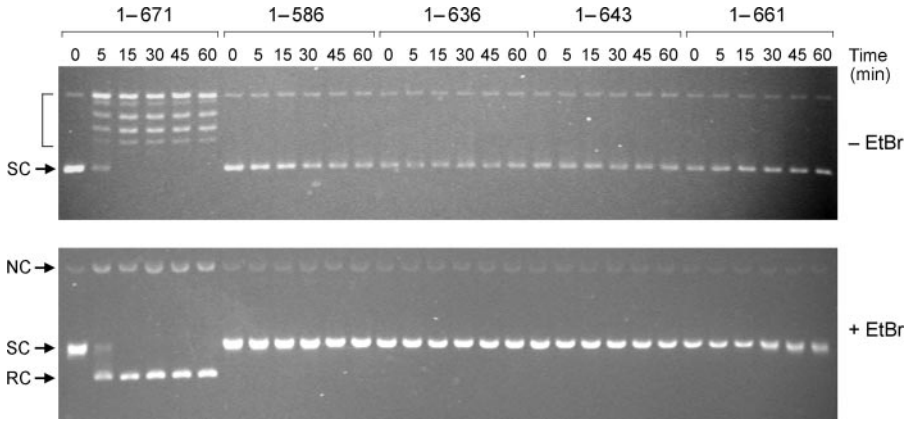

FIGURE 7. **Effect of BRCT deletions on AMP-dependent relaxation of plasmid DNA.** Reaction mixtures (160 μl) containing 20 mM Tris-HCl (pH 8.0), 5 mM $MgCl_2$, 2 mM dithiothreitol, 10 mM AMP, 2.4 μg (1.4 pmol) of supercoiled pUC19 DNA, and 26 μg of (340 pmol) of the indicated LigA preparation were incubated at 22 °C. Aliquots (20 μl) were withdrawn at the times specified and quenched immediately by adjustment to 0.8% SDS, 20 mM EDTA, and 4% glycerol. The time 0 sample was taken prior to the addition of ligase. The quenched reactions were split into two 10-μl aliquots, which were analyzed in parallel by electrophoresis through horizontal 1% agarose gels containing Tris-glycine buffer (*top panel*) or Tris-glycine buffer and 0.5 μg/ml EtBr (*bottom panel*). The gel in the *top panel* was soaked in a 0.5 μg/ml EtBr solution for 30 min. The supercoiled (*SC*), relaxed circle (*RC*), and nicked circle (*NC*) forms of the plasmid DNA are indicated at *left*. Topoisomers of relaxed plasmid DNA are indicated by *brackets* in the *top panel*.

not shown), indicating that the observed activity was not attributable to a contaminating topoisomerase. The instructive findings were that deletion of all or part of the BRCT domain abolished AMP-dependent supercoil relaxation (Fig. 7). Because the BRCT domain is not poised near the active site, it is unlikely that BRCT deletion affects the chemical steps of the reverse step 3 reaction; rather, we hypothesize that BRCT deletion adversely affects the formation or longevity of the AMP·LigA·DNA ternary complex.

Alanine Mutations of the BRCT Domain—We targeted for alanine scanning conserved basic side chains located on the surface of the *Thermus* LigA BRCT domain. We chose four basic residues (Arg^{614}, Lys^{627}, Lys^{634}, and Lys^{635} in *E. coli* LigA) projecting out from the same face of the BRCT domain (Fig. 6*B*) that we considered plausible candidates to engage in DNA contacts or interdomain interactions. To test this idea, we introduced a single-alanine mutation in lieu of Arg^{614} and Lys^{627} and a double-alanine substitution at vicinal residues Lys^{634} and Lys^{635}. We extended the alanine scan to two other basic residues, Lys^{648} and Lys^{651} in *E. coli* LigA, that are conserved in *Thermus* and *Mycobacterium* LigA (Fig. 6*A*). Lys^{648} is located in the second α helix and makes a bifurcated hydrogen bond to two main chain carbonyls in the surface loop preceding the helix (Fig. 6*B*). Lys^{651} makes a hydrogen bond to a main chain carbonyl in the third β strand (Fig. 6*B*). The mutants were purified (Fig. 6*C*) and assayed for nick sealing (Fig. 6*D*). The alanine substitutions elicited decrements on LigA specific activity as follows: R614A (14% of wild-type activity); K627A (40%); K634A-K635A (44%); K648A (37%); K651A (35%). None of the alanine mutants phenocopied the severe effects of deleting the BRCT domain.

Previously, Feng *et al.* (22) reported the effects of missense mutations at 12 amino acids of the BRCT domain of LigA from *Thermus* species AK16D, corresponding to Thr^{606}, Arg^{614}, Gly^{625}, Lys^{627}, Ser^{631}, Val^{632}, Gly^{642}, Gly^{646}, Lys^{648}, Ala^{652}, Leu^{655}, and Glu^{663} in *E. coli* LigA. The *Thermus* equivalents of *E. coli* LigA Lys^{627} and Lys^{648} were replaced conservatively by arginine, which had no apparent effect on LigA activity (22). The Arg^{614} equivalent was substituted by alanine, which reduced *Thermus* LigA nick sealing activity to ~60% of the wild-type level (22). Thus, to the limited extent that the present and prior mutational analyses overlap, the results are fairly concordant and illustrate the modest contributions of the basic side chains (lysine or arginine) at positions 614, 627, and 649 in *E. coli* LigA. Of the other mutations studied by Feng *et al.* (22), the only ones that were seriously deleterious were Gly-to-Ile changes at the equivalents of *E. coli* LigA residues Gly^{625} and Gly^{642}. Reference to the BRCT domain structure (Fig. 6*B*) indicates that both glycines are located at transitions from ordered secondary structures to loops, suggesting that the adverse effects of the bulky Gly-to-Ile mutations might have resulted from distortions of the BRCT fold.

Taken together, these data suggest that the essentiality of the LigA BRCT domain, whether due to its putative interactions with the DNA or other component domains of LigA, entail contributions from multiple functional groups. The *Thermus* LigA BRCT domain can fit in the crystal lattice of DNA-bound *E. coli* LigA in the cavity presumed to be occupied by the *E. coli* BRCT domain, for which no workable electron density was observed. This places the BRCT domain on the 5′-PO_4 side of the nicked duplex, where it could bridge the surfaces of the NTase and HhH domains and thereby extend the protein clamp around the DNA.

Effects of Missense Mutations on Supercoil Relaxation—We surveyed several of the missense mutants for their ability to relax supercoiled DNA in the presence of AMP (Fig. 8). The HhH domain mutants D450A, R510A, E519A, and D551A retained DNA relaxation function, concordant with their ability to effectively ligate nicks. By contrast, valine substitutions at each of the four targeted glycines of the HhH domain (Gly^{455}, Gly^{489}, Gly^{521}, and Gly^{553}) eliminated supercoil relaxation activity. Alanine substitutions at three of these HhH glycines (Gly^{455}, Gly^{489}, and Gly^{533}) slowed the rate of relaxation by about an order of magnitude when compared with wild-type LigA, whereas the G521A change virtually eliminated supercoil relaxation. Thus, the hierarchy of HhH glycine mutational effects of relaxation paralleled that observed for nick sealing. Relaxation was also enfeebled by the R446A and R487A changes in the HhH domain that reduced nick ligation specific activity to 5–6% of wild-type LigA. The OB domain mutations R333A and R379A strongly suppressed DNA relaxation (Fig. 8), consistent with their impact on nick sealing. Several other OB domain mutations slowed the rate of supercoil relaxation, with relative rates as follows: V383A → I384A → T334A or Q330A

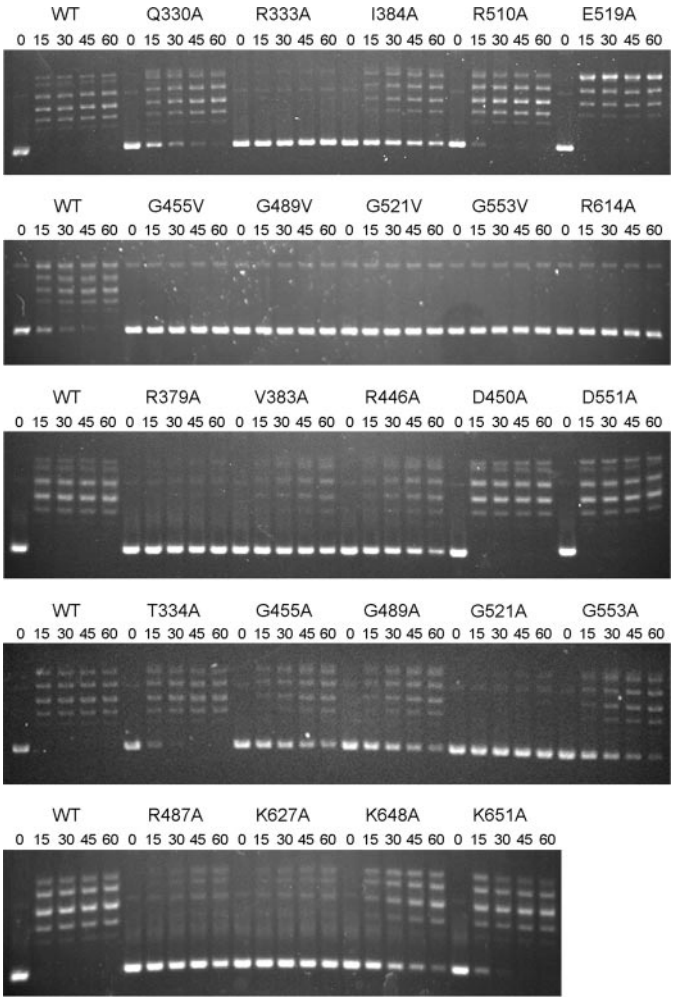

FIGURE 8. **Effect of missense mutations on AMP-dependent supercoil relaxation.** Reaction mixtures (120 μl) containing 20 mM Tris-HCl (pH 8.0), 5 mM $MgCl_2$, 2 mM dithiothreitol, 10 mM AMP, 1.8 μg (1 pmol) of supercoiled pUC19 DNA, and 6 μg (79 pmol) of the indicated LigA preparation were incubated at 22 °C. Aliquots (20 μl) were withdrawn at the times specified and quenched immediately. The time 0 sample was taken prior to the addition of ligase. Aliquots (10 μl) were analyzed by electrophoresis through horizontal 1% agarose gels containing Tris-glycine buffer. The gels were soaked in a 0.5 μg/ml EtBr solution for 30 min and then photographed with UV transillumination. *WT*, wild type.

(Fig. 8). The BRCT domain mutations R614A and K627A strongly suppressed supercoil relaxation; K648A slowed relaxation by about an order of magnitude and K651A had little effect (Fig. 8).

Conclusions—By using the crystal structure of the LigA·DNA-adenylate complex to guide mutational analyses of the OB and HhH domains, we defined functionally relevant components of the DNA-binding surface and amino acids that aid in forming the C-shaped protein clamp around the DNA helix. Studies of the LigA BRCT domain highlight its necessity for nick sealing.

REFERENCES

1. Little, J. W., Zimmerman, S. B., Oshinsky, C. K., and Gellert, M. (1967) *Proc. Natl. Acad. Sci. U. S. A.* **58,** 2004–2011
2. Gumport, R. I., and Lehman, I. R. (1971) *Proc. Natl. Acad. Sci. U. S. A.* **68,** 2559–2563
3. Olivera, B. M., Hall, Z. W., and Lehman, I. R. (1968) *Proc. Natl. Acad. Sci. U. S. A.* **61,** 237–244
4. Singleton, M. R., Håkansson, K., Timson, D. J., and Wigley, D. B. (1999) *Structure* (*Camb.*) **7,** 35–42
5. Lee, J. Y., Chang, C., Song, H. K., Moon, J., Yang, J., Kim, H. K., Kwon, S. T., and Suh, S. W. (2000) *EMBO J.* **19,** 1119–1129
6. Gajiwala, K. S., and Pinko, C. (2004) *Structure* (*Camb.*) **12,** 1449–1459
7. Srivastava, S. K., Tripathi, R. T., and Ramachandran, R. (2005) *J. Biol. Chem.* **280,** 30273–30281
8. Nandakumar, J., Nair, P. A., and Shuman, S. (2007) *Mol. Cell* **26,** 257–271
9. Sriskanda, V., Moyer, R. W., and Shuman, S. (2001) *J. Biol. Chem.* **276,** 36100–36109
10. Sriskanda, V., and Shuman, S. (2002) *J. Biol. Chem.* **277,** 9685–9700
11. Benarroch, D., and Shuman, S. (2006) *Virology* **353,** 133–143
12. Sriskanda, V., Schwer, B., Ho, C. K., and Shuman, S. (1999) *Nucleic Acids Res.* **27,** 3953–3963
13. Zhu, H., and Shuman, S. (2005) *J. Biol. Chem.* **280,** 12137–12144
14. Shuman, S., and Lima, C. D. (2004) *Curr. Opin. Struct. Biol.* **14,** 757–764
15. Timson, D. J., and Wigley, D. B. (1999) *J. Mol. Biol.* **285,** 73–83
16. Kaczmarek, F. S., Zaniewski, R. P., Gootz, T. D., Danley, D. E., Mansour, M. N., Griffor, M., Kamath, A. V., Cronan, M., Mueller, J., Sun, D., Martin, P. K., Benton, B., McDowell, L., Biek, D., and Schmid, M. B. (2001) *J. Bacteriol.* **183,** 3016–3024
17. Lim, J. H., Choi, J., Kim, W., Ahn, B. Y., and Han, Y. S. (2001) *Arch. Biochem. Biophys.* **388,** 253–260
18. Jeon, H. J., Shin, H. J., Choi, J. J., Hoe, H. S., Kim, S. K., Suh, S. W., and Kwon, S. T. (2004) *FEMS Microbiol. Lett.* **237,** 111–118
19. Wilkinson, A., Smith, A., Bullard, D., Lavesa-Curto, M., Sayer, H., Bonner, A., Hemmings, A., and Bowater, R. (2005) *Biochim. Biophys. Acta* **1749,** 113–122
20. Lu, J., Tong, J., Feng, H., Huang, J., Afonso, C. L., Rock, D. L., Barany, F., and Cao, W. (2004) *Biochim. Biophys. Acta* **1701,** 37–48
21. Sriskanda, V., and Shuman, S. (2001) *Nucleic Acids Res.* **29,** 4930–4934
22. Feng, H., Parker, J. M., Lu, J., and Cao, W. (2004) *Biochemistry* **43,** 12648–12659
23. Srivastiva, S. K., Dube, D., Kushkal, V., Jha, A. K., Hajela, K., and Ramachandran, R. (2007) *Proteins* **69,** 97–111
24. Liu, P., Burdzy, A., and Sowers, L. C. (2004) *Nucleic Acids Res.* **32,** 4503–4511
25. Modrich, P., Lehman, I. R., and Wang, J. C. (1972) *J. Biol. Chem.* **247,** 6370–6372